

Proton Affinities of Didehydroporphyrin and Subporphyrin in Ground and Excited States Obtained by Quantum Chemical Calculations*

Zoran Glasovac, Mario Vazdar, and Davor Margetić**

Laboratory for Physical Organic Chemistry, Division of Organic Chemistry and Biochemistry, Ruder Bošković Institute, Bijenička cesta 54, HR-10000 Zagreb, Croatia

RECEIVED SEPTEMBER 4, 2008; REVISED NOVEMBER 28, 2008; ACCEPTED DECEMBER 1, 2008

Abstract. Quantum-chemical calculations were used to investigate molecular and electronic properties of porphyrin and subporphyrin. Their basicities were estimated in ground and excited states. It was found that multiple proton - nitrogen lone-pair coordination plays an important role in acid/base properties of the studied molecules. Lone pair-lone pair interactions in didehydroporphyrin and energetic stabilization of its protonated form lead to the increase of a proton affinity compared to porphyrin by 18 kcal mol⁻¹. A planarization of the protonated (dehydroporphyrin) structure leads to the complete reversal of the π -electron ring currents indicating aromaticity of the protonated form. On the other hand, calculations indicate that subporphyrin is slightly (by 5 kcal mol⁻¹) more basic than porphyrin, which was explained by non-planar geometry, imposed by smaller ring size.

Keywords: DFT calculations, NICS, TDDFT, proton affinity, basicity

INTRODUCTION

Design of novel superbases represent important scientific target nowadays¹⁻¹⁰ and many efforts has been laid in developing building blocks that can be combined together ending up in highly basic molecule. Special emphasis has been directed to the structures possessing two or more basic centers capable of formation of intramolecular hydrogen bond which can significantly enhance basicity of considered system.²⁻⁴ Special case of such systems are the rigid structures with basic centers brought to the close proximity where strong lone pair - lone pair repulsion occurs in neutral form. It is well known that such repulsion, in conjunction with hydrogen bond formation upon protonation, is responsible for the unusually high basicity of archetypal proton sponge – DMAN.⁵ This logic was used as the general idea in design of a number of proton sponges (TMGN,^{6,7} vinimidines,⁸ polypyridines,⁹ Verkade bases,¹⁰ etc.¹¹).¹²

Cyclic tri- and tetrapyridines are known for their very high gas-phase basicity.¹³ By replacing pyridines with dehydropyrrole subunits, large polycyclic structures similar to porphyrin¹⁴ and subporphyrin could be designed. As the structural relatives of aforementioned pyridine derivatives, didehydroporphyrin and its analogues represent good candidates for novel superbases.

Porphyrins are thoroughly investigated, both experimentally and computationally, while the literature data on didehydroporphyrin is rather scarce. There are only two computational papers dealing with didehydroporphyrin.^{15,16} However, no information on the basicity either of porphyrines or didehydroporphyrines can be found in literature.

Due to the characteristic electron ring currents in porphyrin analogues,¹⁷ electronic excitation, *i.e.* charge redistribution caused by electronic transition, can also significantly modify the acid-base properties of these compounds. Computational investigation of excited state proton transfer (as an important process in biological systems) has been applied for many biologically important molecules such as guanine¹⁸ and related species.¹⁹ Gas phase basicities in the excited states of organic molecules have been previously calculated at different computational levels.²⁰⁻²² Proton affinities in the excited states for 1,5- and 1,8-diaminonaphthalenes were successfully computed using ground state B3LYP/6-31G(d,p) calculations in conjunction with CIS/6-31G(d,p) approach for the determining vertical excitation energies.²³

The aim of this computational study is to assess proton affinities of hypothetical porphyrin derivatives²⁴ such as didehydroporphyrin (**P**), dehydroporphyrin

* Dedicated to Professor Zvonimir Maksić on the occasion of his 70th birthday.

** Author to whom correspondence should be addressed. (E-mail: margetid@emma.irb.hr)

(**HP**) and subporphyrin (**P2**) (Figure 1) in ground and excited states. Didehydroporphyrin **P** was specifically chosen with an assumption that basicity will be greatly increased by the coordination of one proton with four nitrogens in the centre of porphyrin core. Furthermore, subporphyrin **P2**, a molecule closely related to subphthalocyanines,²⁵ was chosen on the premise that the reduction of the size of porphyrin ring by one pyrrole moiety will bring the remaining nitrogen atoms to the closer distance and increase the repulsion between lone pairs within the central part of subporphyrin moiety.

COMPUTATIONAL DETAILS

Geometries of all species were optimized using HF/6-31G(d)²⁶ method as implemented in Gaussian 03 suite of programs.²⁷ All minima were verified by vibrational analysis (no imaginary frequencies were obtained). Zero point vibrational energies (ZPVE) were corrected using scaling factor $f = 0.8925$ according to literature recommendation.²⁸ More accurate electronic energies (E_{el}) were obtained by conducting single point MP2(fc)//6-311+G(d,p) calculations at the HF/6-31G(d) optimized geometries (hereafter denoted as MP2 model). Time dependent density functional calculations (TDDFT)²⁹ were performed using B3LYP functional in conjunction with 6-31G(d) basis set at the HF/6-31G(d) optimized structures to obtain the lowest vertical excitation energies. Aromaticity of studied species was estimated by NICS values recommended by Schleyer and coworkers,³⁰ calculated at the GIAO/B3LYP/6-311+G(d,p)//6-

31G(d) level. NICS values were calculated at 1 Å above the ring centers to minimize influence of strong para-tropic ring currents.

RESULTS AND DISCUSSION

Ground State Geometries

Optimized ground state structures calculated at the HF/6-31G(d) level are shown in Figures 2 and 3. In spite of rather low level of theory employed for calculating geometries, rigidity of the structures prevents significant conformational changes of the investigated molecules. Generally, geometries optimized at the HF/6-31G(d) level of theory are sufficiently accurate for predicting properties of molecules like PAs³¹ and NICS³⁰ as long as sufficiently accurate single point electronic energies are calculated. For this purpose we employed B3LYP or MP2 methods in conjunction with 6-311+G(d,p) basis set what ensures sufficient accuracy of the calculated PA(MP2) and NICS values.

As expected, porphyrin structure **H₂P** is highly symmetrical and planar, protonation of which leads to the slightly distorted **H₃P** (Figure 2). Two different structures were located for subporphyrin (**P2**), in further discussion designated by **P2a** and **P2b**. While **P2a** is more stable structure, **P2b** is structurally similar to the protonated **HP2** so both structures are considered in further discussion. Structures obtained for **P** (Figure 2), **P2a** and **P2b** (Figure 3) possess bowl-shaped geometries, which resemble curved- π surfaces of polyaromatics such as fullerenes, corannulene,³² hemifullerene^{33–35} and subphthalocyanine.^{36,37} This structural features could be ascribed to the unfavorable interactions of the nitrogen lone pairs directed to each other which is reduced by deviation of the structures from planarity. Protonation of **P** leads to the planar **HP** (Figure 2), while in the case **P2a** and **P2b** no planarization occurs presumably due to the smaller ring size in the latter structures.

Didehydroporphyrin **P** has non-planar, bowl-shape, twisted structure. In this structure, four pyrrole rings have alternating orientations inwards/outwards in relation to the central ring (in-out-in-out). This orientation causes asymmetry in the structure, where pyrrole rings possess unsymmetrical bond lengths. Methylidene bridges bond lengths are remarkably different (1.470 and 1.334 Å), as compared to the average bond length of porphyrin **H₂P** (1.387 Å). The structural details of particular interest in the series of porphyrin species depicted in Figure 2 are N(1)H(1)–N(2) distances. In the structure of **HP**, proton is attached to one of the pyrrole nitrogen atoms and the contact distance between hydrogen atom and the adjacent pyrrole nitrogen

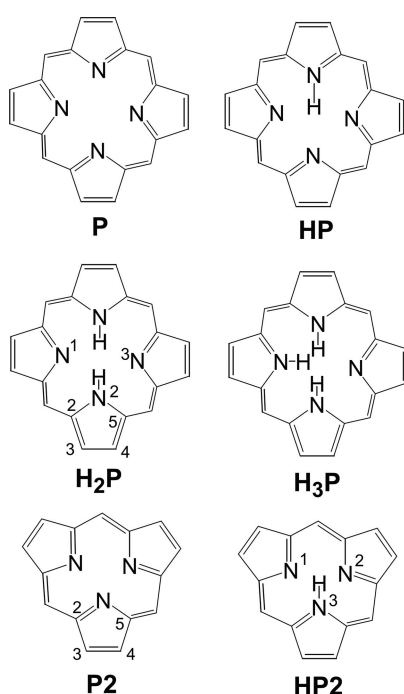


Figure 1. Schematic representation of investigated molecules.

(N(1)H(1)–N(2)) is 2.257 Å. This distance is by 0.054 Å shorter than the value calculated for **H₂P** (2.311 Å). However, bond distance between proton and nitrogen atom positioned at opposite pyrrole subunit is 3.040 Å indicating practically no interaction. Analysis of the bond lengths in the protonated porphyrin **H₃P** reveals considerably shorter N(1)H(1)–N(2) distance with respect to the one in **H₂P** (2.242 Å). This is due to the presence of three partially positive hydrogen atoms in close proximity inducing their bending toward the electron rich lone pair as well as increasing in dipole strength due to the introduction of positive charge.

An isomer **P2a** has unsymmetrical structure, where two pyrrole rings are pointing outwards with the third pyrrole is pointing inwards. Alternate structure of **P2a** closely resembles to the one found in *N,N,N'*-tris(*p*-tolyl)azacalix[3](2,6)pyridine, possessing three pyridine N atoms which are trying to avoid a destabilizing overlap of the lone electron pairs of N_{py} atoms.⁹ On the other hand, **P2b** isomer has symmetrical structure, with three pyrrole rings pointing outwards of the central ring plane. A symmetrical structure **P2b** is predicted to be less stable by 12.6 kcal mol⁻¹ over **P2a**. Calculations of protonated forms of both isomers led to the single minima **HP2**. The concave structure of **HP2** resembles the one of **P2b**, with three pyrrole rings and NH proton pointing outwards of the central ring plane. However, this structure is unsymmetrical and NH proton is not located in the centre of the ring. The N(1)–N(2) and N(2)–N(3) bond lengths in **HP2** are 2.509 and 2.580 Å, respectively, while protonated *N,N,N'*-tris(*p*-tolyl)-azacalix[3]-[2,6]pyridine⁹ has intermediate N(1)–N(2) and N(2)–N(3) bond length values of 2.534 and 2.566 Å. A proton is attached to one of the pyrrole nitrogen atoms (the N(1)–H(1) bond length is 1.011 Å), while the contact distance between hydrogen atom and the adjacent pyrrole nitrogen H(1)–N(2) is 1.798 Å. These hydrogen bond lengths are somewhat longer than the one of 1,8-bis(dimethylamino)naphthalene:⁹ N(1)–H(1) bond length was 1.191 Å and the N(2)–H(1) distance was 1.451 Å, which is a consequence of rigid cyclic structure. On the other hand, N(2)–H(1) distance in **HP2** is more similar to the corresponding interatomic distance found in *N,N,N'*-tris(*p*-tolyl)azacalix[3]-[2,6]pyridine. In this molecule N(1)–H(1) bond length was 1.187 Å, while the N(2)–H(1) distance was 1.634 Å, which is much shorter than the sum of the van der Waals radii of H and N atoms (2.75 Å).⁹ The N(2)–H(1) bond length in **HP2** indicates the existence of intramolecular hydrogen bonding, where proton is shared by three N atoms.

Although the protonation of **P2** occur in the σ plane, formed positive charge is shifted away from the protonation site. Comparison of Mulliken net charges of

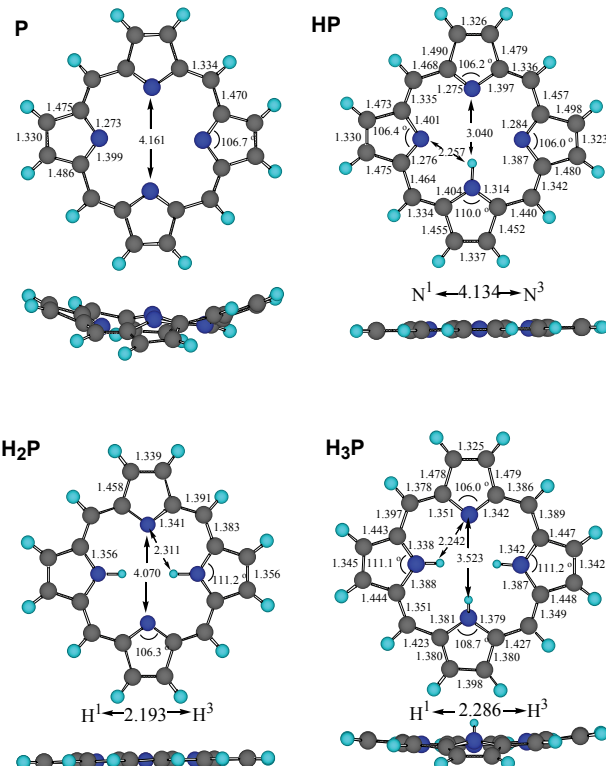


Figure 2. HF/6-31G(d) structures of **P**, **HP**, **H₂P** and **H₃P** (distances are given in Å, and angles in °), top and side-views.

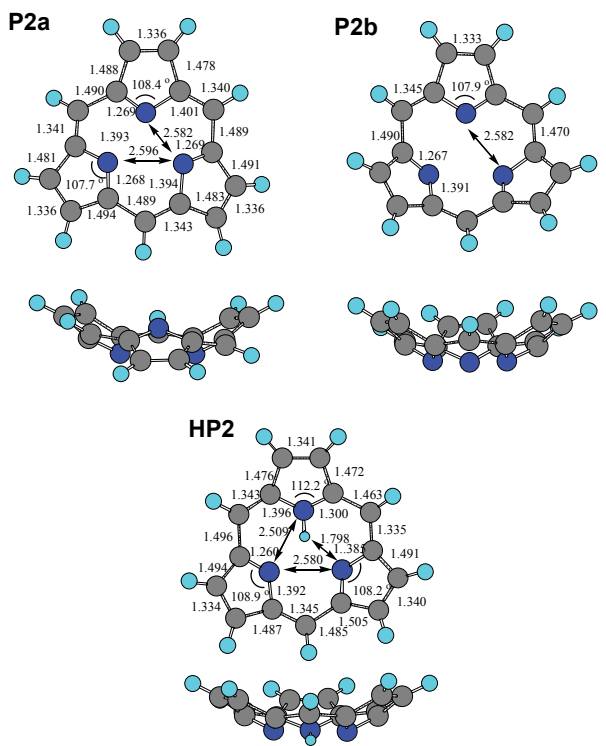


Figure 3. HF/6-31G(d) structures of **P2a**, **P2b** and **HP2** (distances are given in Å, and angles in °), top and side-views.

P2 conformers and their protonated form **HP2**, calculated at the B3LYP/6-311+G(d,p)//HF/6-31G(d) level of theory, reveals an increase in positive charge (by 0.4 atomic charge units, *e*). This increase is especially pronounced at the tertiary carbon atoms C(2) and C(5) within the pyrrole subunit. Furthermore, significant decrease in negative charge (by 0.2 *e*) is observed at the outer carbon atoms C(3) and C(4). Similar trend is observed for other investigated cyclic polypyrroles, being more pronounced in dehydroporphyrin **HP** than in porphyrin **H₂P**. An inspection of electrostatic potential isosurfaces (Figures 4 and 5) leads to the similar conclusion. Rather high electron density is found at the outer atoms while the central part of the molecule is slightly electron deficient. Positive charge, which was introduced by protonation of **P2** compensates relative high electron density throughout the whole molecule. However, it is interesting to note that the change is asymmetrical in nature, meaning that on the concave side of the bowl-shaped protonated **HP2** the decrease in negative electrostatic potential is much smaller than on the convex side.

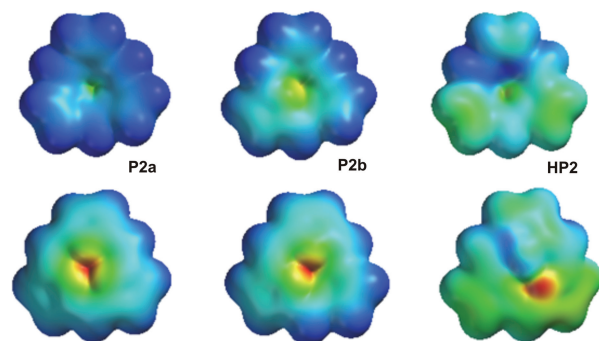


Figure 4. Electrostatic potential plotted on electron density isosurface (isovalue = 0.002 electrons/ a_0^3 ; a_0 , bohr – atomic unit of length) for **P2a**, **P2b** and **HP2** (top row concave, bottom row convex side). Electron rich and electron poor regions are given in blue and red colors, respectively.

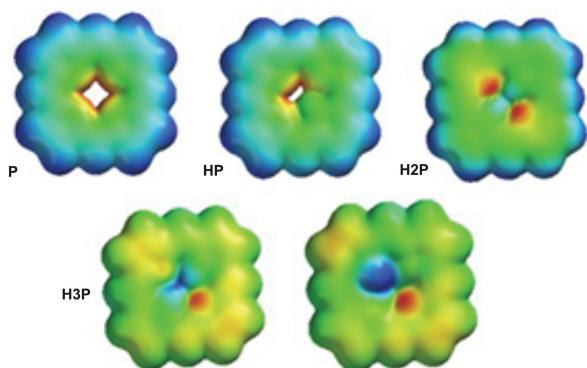


Figure 5. Electrostatic potential plotted on electron density isosurface (isovalue = 0.002 electrons/ a_0^3) for **P**, **HP**, **H₂P** and **H₃P** (concave and convex side). Electron rich and electron poor regions are given in blue and red colors, respectively.

Basicities as Assessed by Proton Affinities

Proton affinities at the scaled HF and MP2 levels of theory ($\text{PA}(\text{HF}_{\text{sc}})$) were obtained according to computational methodology established by Maksić and coworkers.^{38,39}

$$\text{PA}(\text{HF}_{\text{sc}}) = 0.8924 \cdot \Delta E_{\text{el}}(\text{HF}) + 10.4 \quad (1)$$

(expressed in kcal mol⁻¹), where

$$\Delta E_{\text{el}}(\text{HF}) = E_{\text{el}}(\text{neutral}) - E_{\text{el}}(\text{protonated}) \quad (2)$$

and

$$\text{PA}(\text{MP2}) = E_{\text{tot}}(\text{MP2})_{\text{B}} - E_{\text{tot}}(\text{MP2})_{\text{BH}^+} \quad (3)$$

where subscripts B and BH^+ indicate neutral and protonated forms, respectively.

We have recently shown that MP2//HF approach described in Eq. (3) correctly predict gas-phase proton affinities for series of guanidines possessing intramolecular hydrogen bonds.³¹ This approach is considered to be sufficiently accurate also for porphyrine bases. Additionally, PAs at the HF_{sc} level of theory are given for comparative purposes (Table I). The largest PA value obtained by HF_{sc} method is for **P** (262.3 kcal mol⁻¹), while MP2 approach predicts the largest PA for molecule **P2b** (258.8 kcal mol⁻¹). Differences obtained by two methods may be explained by more accurate treatment of the hydrogen bonding by MP2 calculations.

Presence of unfavorable repulsion between nitrogen lone pairs, similar to that in proton sponges, exist in both **P** and **P2** being significantly more pronounced in the latter. Therefore, an increase of PA of **P** with respect to the **H₂P** could be easily explained in terms of the lone pair protonation effect. This is further corroborated by comparison of PA of **P** to the PA values of **P2a** and **P2b**. While in **P2b** three nitrogen atoms possess lone pairs directed to each other in **P2a** one nitrogen is oriented in a way which minimizes lone pair interactions. This geometry reorganization leads to a higher stability of **P2a** with respect to **P2b** and consequently to the lower PA by 15.6 kcal mol⁻¹. It should be recalled here that protonation of both neutral structures **P2a** and **P2b** leads to the same geometry. This result indicates significant contribution of the third pyrrole lone pair to the overall proton coordination. Second point that should be emphasized is deviation from planarity in investigated systems. Highly delocalized electron density present in porphyrine-like structures tends to preserve planar geometry. However, in **P2a** and **P2b** deviation from planarity of π -electron system introduces an important destabilization effect. Similar, but smaller devia-

Table 1. Electronic (E_{el}) and total energies (E_{tot}), zero point vibrational energies (ZPVE) and ground state proton affinities of studied molecules

Mol.	$E_{el}(\text{HF})^{(a)}$ [$E_{el}(\text{MP2})$]	ZPVE ^(a)	$[E_{tot}(\text{MP2})]^{(a)}$ [$\text{PA}(\text{HF}_{sc})^{(b)}$ [$\text{PA}(\text{MP2})]^{(b),(c)}$]
H₂P	-983.25693	0.31901	235.3 [-986.90474]
			[-986.62002] [238.6]
H₃P	-983.65837	0.33064	
	[-987.29534]		[-987.00024]
P	-981.97875	0.29145	262.3 [-985.56463]
			[-985.30451] [256.9]
HP	-982.42828	0.30653	
	[-985.98754]		[-985.71396]
P2a	-736.41011	0.21765	250.5 [-739.11887]
			[-738.92462] [243.2]
P2b	-736.39007	0.21701	261.7 [-739.09349]
			[-738.89980] [258.8]
HP2	-736.83862	0.23237	
	[-739.51953]		[-739.31214]

^(a) Expressed in hartrees.^(b) Expressed in kcal mol⁻¹ (1 kcal = 4.184 kJ).^(c) Calculated according Eq. (3).

tion from planarity is also observed in **P**. While protonation of **P** leads to the complete macrocycle ring planarization, in tripyrrole derivatives **P2a** and **P2b** planarization cannot be achieved due to smaller ring size. These results indicate the most efficient relaxation-upon-protonation effect in **P-HP** acid-base pair. In the other calculated structures lone pair interaction in the neutral form was not observed (**H₂P-H₃P**), or steric relaxation was not achieved due to a small ring size (**P2a-HP2**).

To obtain better insight in the role of intramolecular hydrogen bonding on PAs, we compared the results of calculated gas-phase PAs of the investigated cyclic polypyroles with analogous compounds. Experimental gas-phase PAs of pyridine and imidazole are 222.0 and 225.3 kcal mol⁻¹, respectively. Furthermore, incorporation of two imidazole rings in rigid structure such as Schwesinger proton sponge resulted in a large increase of basicity. Calculations at the HF/6-31G(d) level of theory yielded PA of 269.5 kcal mol⁻¹. Similarly, calculations of linear dihydroaminotripyrrole predicted large PA(HF_{sc}) of \approx 270 kcal mol⁻¹.² It should be noted that in linear tripyrroles nitrogen atoms are situated in 1,4-fashion separated by double bonds and they were not actually centers of protonation. Recently, Maksić and coworkers obtained the PAs of two cyclic tetrakispyridines (286.0 and 291.4 kcal mol⁻¹), using DFT approach.⁴⁰ While the PAs of compounds investigated in this paper are significantly lower than these of polypyridines, they are of comparable basicity to guanidines and can be considered as the strong neutral organic bases.

Proton Affinities of Porphyrins in a First Excited State

Excited state proton transfer is the foundation of a number of papers dealing with light induced molecular motors and/or switches.⁴¹ As the porphyrins are efficient light harvesting molecules,⁴² it is of a considerable interest to analyze their proton affinities in excited states. For a calculation of excited state proton affinities, the Förster cycle approach^{43,44} was used. It should be stressed that it considers only vertical excitation processes since they are much faster compared to the proton transfer. The lowest excitation energies were obtained by time-dependent density function theory method⁴⁵ (TDDFT) in conjunction with the B3LYP functional (TD-B3LYP) and the 6-31G(d) basis set. Lowest vertical excitation energies were calculated by using the HF/6-31G(d) geometries. The results are summarized in Table 2. Excitation energies and excited states proton affinities of studied molecules are collected in Table 2. The examination of results has revealed that both computational methods (PA(HF)_{exc} and PA(MP2)_{exc}) predict that molecule **P** has the largest excited state proton affinity (280.8 kcal mol⁻¹ and 275.5 kcal mol⁻¹ at HF and MP2 levels, respectively), while **P2a** the smallest. Adiabatic excitation energies of studied molecules unfortunately were not obtained due to a large number of very shallow local minima connected to the numerous energetically close electronic transitions.

The results collected in Table 2 also show that basicities of all species are predicted to be higher in the excited state. The only exception is **P2a** having smaller basicity than in the ground state. This trend has been previously observed,^{46,47} and it can be attributed to the different charge distribution in the excited state with respect to the ground state.⁴⁷

Table 2. Lowest excitation energies^(a) and excited states proton affinities obtained by TDDFT/B3LYP/6-31G(d)//HF/6-31G(d) method^(a) and Förster cycle^{43,44}

	E_{exc} /eV	$\text{PA}(\text{HF})_{exc}^{(b)}$	$\text{PA}(\text{MP2})_{exc}^{(b)}$
P	1.86	280.8	275.5
HP	1.18		
H₂P	2.47	237.6	240.9
H₃P	2.38		
P2a	1.17	247.6	240.3
P2b	1.79	273.1	270.1
HP2	1.29		

^(a) For all molecules $\pi-\pi^*$ transitions were found to be of lowest energy (in the case of **H₂P** the state symmetry is B_{3u}).^(b) Expressed in kcal mol⁻¹. $\text{PA}(\text{HF})_{exc} = \text{PA}(\text{HF}_{sc}) + \Delta E_{exc}$; $\text{PA}(\text{MP2})_{exc} = \text{PA}(\text{MP2}) + \Delta E_{exc}$.

Aromaticity

Finally, in order to gain more insight into the molecular and electronic properties of studied molecules, their aromaticity was estimated by calculations of nucleus-independent chemical shifts (NICS)^{30,48} according to the computational formalism developed by Schleyer and results presented in a Table 3. NICS values were calculated at 1 Å above the center of the molecule (global aromaticity), and also above the centre of one of the pyrrole rings (local aromaticity). The calculations of the NICS values show another interesting feature of the dehydroporphyrins and subporphyrins. The NICS value of the subporphyrin **P2a** was not calculated due to a significant contribution of the nitrogen lone pairs on the both sides of the ring. It is known that porphyrins possess negative NICS values which indicate their aromatic character.⁴⁹ These results agree well with their 22π electronic structure. Didehydroporphyrin **P** possesses 24π electron system which according to the Hückel's rule should be antiaromatic, which in turn was predicted by positive NICS value (11.8 ppm). Almost identical positive number was obtained for the subporphyrin **P2b** (11.9 ppm), indicating an antiaromatic structure. This result is opposite to the expected aromatic character of 18π electron structure, which may be explained by non-planarity of **P2b** and the lack of efficient π -conjugation. It should be noted that similar antiaromatic NICS values were found at 2 and 3 Å above ring center inside cavity as well as at 1 Å at the outer side. An additional increase in antiaromaticity of **P2b** was observed upon protonation. This is not surprising having in mind the fact that there is no significant geometrical and electronic change on going from **P2b** to **HP2**. On the other hand, protonation of didehydroporphyrin **P** leads to the complete reversal of the magnetic properties of the molecule. NICS value of **HP** (-13.0 ppm) indicates significant π -diatropic current and aromatic character. Again, no significant change in pyrrole geometry was observed, apart from complete planarization of **P** molecule as mentioned earlier. Although nitrogen lone pairs

do not significantly contribute to the overall π electron density, the planarization obviously plays an important role.

Results obtained for global and local aromaticity in porphyrin **P** are in accordance with results published by Schleyer⁴⁸ NICS values of **P** indicate that pyrrole rings with NH groups are more aromatic (NICS = -15.2 ppm, almost identical to pyrrole: -15.1 ppm)³⁰ than the other five-membered rings (NICS = -4.5 ppm). Furthermore, NICS value obtained for pyrrole ring incorporated in **P2b** (NICS = -5.7 ppm) indicates that pyrrole rings in **P2b** are less aromatic than isolated pyrrole itself.

CONCLUSION

The examination of the basicity of porphyrin **H₂P** and its tripyrrole analogue subporphyrin **P2** describes the importance of multiple nitrogen lone-pair coordination of proton in designing acid/base properties of the molecules. Lone pair-lone pair interaction in neutral base **P** and stabilization of its protonated form lead to the ≈ 18 kcal mol⁻¹ higher **PA** than porphyrin itself. Additionally, planar structure in protonated porphyrine **HP** allows maximal stabilization effect what results in high ground state proton affinity of **P**. On the other hand, **P2a** offers basicity higher than **H₂P** by ca. 5 kcal mol⁻¹. This is consequence of two opposite effects: lack of destabilization caused by lone pair-lone pair repulsion in the neutral form and deviation from planarity what reduces stabilization of the protonated structure by delocalization and resonance. The trend in proton affinities observed in ground state is kept upon excitation. However, a decrease in proton affinities is found in the case of **P2a**. Aromatic character of most of the investigated structures is not affected by protonation except for **P**. In this case, planarization of the protonated structure leads to the complete reversal of the π -electron ring currents indicating change from antiaromatic to aromatic character upon protonation.

Acknowledgements. We thank Professor Maksić to whom this paper is dedicated, for his support, enlightening and stimulating discussions and suggestions over many years. Croatian Ministry of Science, Education and Sport is acknowledged for financial support (projects Nos. 098-0982933-3218 and 098-0982933-2920). We also would like to thank the Computing centre of the Zagreb University for allocating the computing time at the computer cluster Isabella.

REFERENCES

1. R. W. Alder, *Chem. Rev.* **89** (1989) 1215–1223.
2. Z. B. Maksić, I. Despotović, and Z. Glasovac, *J. Phys.*

Table 3. NICS values obtained by GIAO/B3LYP/6-311+G(d,p)//HF/6-31G(d) method

Molecule	NICS/ppm
H₂P	-13.6
H₃P	-13.0
P	11.8
HP	-13.0
P2b (pyrrole)	(-5.7) ^(a)
P2b (center)	11.9
HP2 (center)	18.0

^(a) Center of the pyrrole ring.

- Org. Chem.* **15** (2002) 499–508; B. Kovačević, Z. Glasovac, and Z. B. Maksić, *J. Phys. Org. Chem.* **15** (2002) 765–774.
3. Z. Glasovac, B. Kovačević, E. Meštrović, and M. Eckert-Maksić, *Tetrahedron Lett.* **46** (2005) 8733–8736; M. Eckert-Maksić, Z. Glasovac, P. Trošelj, A. Kütt, T. Roldima, I. Koppel, and I. A. Koppel, *Eur. J. Org. Chem.* **5176**–5184.
 4. V. Raab, E. Gauchenova, A. Merkulov, K. Harms, J. Sundermeyer, B. Kovačević, and Z. B. Maksić, *J. Am. Chem. Soc.* **127** (2005) 15738–15743; Z. Gattin, B. Kovačević, and Z. B. Maksić, *Eur. J. Org. Chem.* (2005) 3206–3213; E. D. Raczyńska, M. K. Cyranski, M. Gutowski, J. Rak, J.-F. Gal, P.-C. Maria, M. Darowska, and K. Duczmal, *J. Phys. Org. Chem.* **16** (2003) 91–106.
 5. H. A. Staab and T. Saupe, *Angew. Chem., Int. Ed.* **27** (1988) 865–879.
 6. V. Raab, J. Kipke, R. M. Gschwind, and J. Sundermeyer, *Chem. Eur. J.* **8** (2002) 1682–1693.
 7. B. Kovačević and Z. B. Maksić, *Chem. Eur. J.* **8** (2002) 1694–1702.
 8. R. Schwesinger, M. Missfeld, K. Peters, and H. G. von Schnerring, *Angew. Chem., Int. Ed.* **26** (1987) 1165–1167.
 9. T. Kanbara, Y. Suzuki, and T. Yamamoto, *Eur. J. Org. Chem.* (2006) 3314–3316.
 10. P. B. Kisanga, B. D'Sa, and J. G. Verkade, *J. Org. Chem.* **63** (1998) 10057–10059; B. Kovačević, D. Barić, and Z. B. Maksić, *New J. Chem.* **28** (2004) 284–288.
 11. D. Margetić, W. Nakanishi, T. Kumamoto, and T. Ishikawa, *Heterocycles* **71** (2007) 2639–2658.
 12. D. Margetić, in: T. Ishikawa (Ed.), *Guanidines, Amidines, and Phosphazenes: Superbases for Organic Synthesis*, Wiley, Chichester, 2009, pp. 9–48.
 13. I. Despotović, B. Kovačević, and Z. B. Maksić, *Org. Lett.* **9** (2007) 1101–1104; I. Despotović, B. Kovačević, and Z. B. Maksić, *Org. Lett.* **9** (2007) 4709–4712; I. Despotović, B. Kovačević, and Z. B. Maksić, *New J. Chem.* **31** (2007) 447–457.
 14. K. Kadish, K. Smith, and R. Guillard (Eds.), *The Porphyrin Handbook*, Academic Press, 1999.
 15. P. Belanzoni, M. Rosi, A. Sgamellotti, L. Bonomo, and C. Floriani, *J. Chem. Soc., Dalton Trans.* **9** (2001) 1492–1497.
 16. T. G. Gantchev, F. Beaudry, J. E. Van Lier, and A. G. Michel, *Int. J. Quantum Chem.* **46**, (1993) 191–210.
 17. E. Steiner and P. W. Fowler, *Org. Biomol. Chem.* **2** (2004) 34–37.
 18. M. K. Shukla and J. Leszczynski, *J. Phys. Chem. A* **109** (2005) 7775–7780.
 19. A. J. A. Aquino, H. Lischka, and C. Haettig, *J. Phys. Chem. A* **109** (2005) 3201–3208.
 20. I. Antol, M. Eckert-Maksić, and H. Lischka, *J. Phys. Chem. A* **108** (2004) 10317–10325.
 21. H. Mishra, S. Maheshwary, H. B. Tripathi, and N. Satyamurthy, *J. Phys. Chem. A* **109** (2005) 2746–2754.
 22. G. A. Ibanez, G. Labadie, G. M. Escandar, and A. C. Oliveri, *J. Mol. Struct.* **645** (2003) 61–68.
 23. K. Takehira, Y. Sugawara, S. Kowase, and S. Tobita, *Photochem. Photobiol. Sci.* **4** (2005) 287–293.
 24. P. Ilić and N. Trinajstić, *Croat. Chem. Acta* **53** (1980) 591–599.
 25. C. G. Claessens, D. Gonzalez-Rodriguez, and T. Torres, *Chem. Rev.* **102** (2002) 835–853.
 26. W. J. Hehre, L. Radom, P. v. R. Schleyer, and J. A. Pople, *Ab initio Molecular Orbital Theory*, Wiley, New York, 1986.
 27. GAUSSIAN 03, Revision B.03, M. J. Frisch, G. W. Trucks, H. B. Schlegel, G. E. Scuseria, M. A. Robb, J. R. Cheeseman, J. A. Montgomery, Jr., T. Vreven, K. N. Kudin, J. C. Burant, J. M. Millam, S. S. Iyengar, J. Tomasi, V. Barone, B. Mennucci, M. Cossi, G. Scalmani, N. Rega, G. A. Petersson, H. Nakatsuji, M. Hada, M. Ehara, K. Toyota, R. Fukuda, J. Hasegawa, M. Ishida, T. Nakajima, Y. Honda, O. Kitao, H. Nakai, M. Klene, X. Li, J. E. Knox, H. P. Hratchian, J. B. Cross, C. Adamo, J. Jaramillo, R. Gomperts, R. E. Stratmann, O. Yazyev, A. J. Austin, R. Cammi, C. Pomelli, J. W. Ochterski, P. Y. Ayala, K. Morokuma, G. A. Voth, P. Salvador, J. J. Dannenberg, V. G. Zakrzewski, S. Dapprich, A. D. Daniels, M. C. Strain, O. Farkas, D. K. Malick, A. D. Rabuck, K. Ravachari, J. B. Foresman, J. V. Ortiz, Q. Cui, A. G. Baboul, S. Clifford, J. Cioslowski, B. B. Stefanov, G. Liu, A. Liashenko, P. Piskorz, I. Komaromi, R. L. Martin, D. J. Fox, T. Keith, M. A. Al-Laham, C. Y. Peng, A. Nanayakkara, M. Challacombe, P. M. W. Gill, B. Johnson, W. Chen, M. W. Wong, C. Gonzalez, and J. A. Pople, Gaussian Inc., Wallingford CT, 2004.
 28. A. P. Scott and L. Radom, *J. Phys. Chem.* **100** (1996) 16502–16513.
 29. E. Runge and E. K. U. Gross, *Phys. Rev. Lett.* **52** (1984) 997–1000.
 30. P. v. R. Schleyer, C. Maerker, A. Dransfeld, H. Jiao, and N. J. R. Van Eikema Hommes, *J. Am. Chem. Soc.* **118** (1996) 6317–6318.
 31. Z. Glasovac, V. Štrukil, M. Eckert-Maksić, D. Schröder, M. Kaczorowska, H. Schwarz, *Int. J. Mass Spectrom.* **270** (2008) 39–46.
 32. T. Kawase and H. Kurata, *Chem. Rev.* **106** (2006) 5250–5273.
 33. R. C. Dunbar, *J. Phys. Chem. A* **106** (2002) 9809–9819.
 34. M. A. Petrukhina and L. Scott, *Dalton Trans.* **18** (2005) 2969–2975.
 35. D. Delaere, M. T. Nguyen, and L. G. Vanquickenborne, *Chem. Phys. Lett.* **333** (2001) 103–112.
 36. N. Kobayashi, *J. Porph. & Phthaloc.* **3** (1999) 453–467.
 37. N. Kobayashi, T. Ishizaki, K. Ishii, and H. Konami, *J. Am. Chem. Soc.* **121** (1999) 9096–9110.
 38. Z. B. Maksić and B. Kovačević, *J. Phys. Chem. A* **102** (1998) 7324–7328.
 39. Z. B. Maksić, B. Kovačević, and D. Kovaček, *J. Phys. Chem. A* **101** (1997) 7446–7453.
 40. B. Kovačević, I. Despotović, and Z. B. Maksić, *Tetrahedron Lett.* **48** (2007) 261–264.
 41. A. L. Sobolewski, *Phys. Chem. Chem. Phys.* **10** (2008) 1243–1247; S. Silvi, A. Arduini, A. Pochini, A. Secchi, M. Tomasulo, F. M. Raymo, M. Baroncini, and A. Credi, *J. Am. Chem. Soc.* **129** (2007) 13378–13379.
 42. M. Kozaki, A. Uetomo, S. Suzuki, and K. Okada, *Org. Lett.* **10** (2008) 4477–4480.
 43. T. Förster, *Naturwissenschaften* (1949) 186–187.
 44. T. Förster, *Z. Electrochem.* **54** (1950) 42–46.
 45. M. K. Shukla and J. Leszczynski, *Int. J. Quantum Chem.* **105** (2005) 387–395.
 46. A. H. Goeller, D. Strehlow and G. Hermann, *ChemPhys-Chem* **6** (2005) 1259–1268.
 47. I. Antol, M. Eckert-Maksić, and M. Klessinger, *J. Mol. Structure (THEOCHEM)* **664–665** (2003) 309–317.
 48. P. v. R. Schleyer and H. Jiao, *Pure Appl. Chem.* **68** (1996) 209–218.
 49. M. K. Cyranski, T. M. Krygowski, M. Wisiorowski, N. J. R. Van Eikema Hommes, and P. v. R. Schleyer, *Angew. Chem., Int. Ed.* **37** (1998) 177–180.

SAŽETAK

Protonski afiniteti didehidroporfirina i subporfirina u osnovnom i pobuđenom stanju dobiveni pomoću kvantnokemijskih računa

Zoran Glasovac, Mario Vazdar i Davor Margetić

*Laboratorij za fizičko-organiku kemiju, Zavod za organsku kemiju i biokemiju,
Institut Ruđer Bošković, Bijenička cesta 54, HR-10000 Zagreb, Hrvatska*

Kvantno kemijski računi provedeni su u svrhu istraživanja molekulskih elektronskih svojstava porfirina i subporfirina. Njihove bazičnosti procijenjene su za osnovno i pobuđena stanja. Pronadena je važna uloga višestruke koordinacije između protona i osamljenog elektronskog para dušika u određivanju kiselo-baznih svojstava proučavanih molekula. Međudjelovanja osamljenih parova u didehidroporfirinu i stabilizacija njegova protonirana oblika dovodi do povećanja protonskog afiniteta u usporedbi s porfirinom za 18 kcal mol^{-1} . Planarizacija protonirane strukture (dehidroporfirina) uzrokuje potpunu promjenu u π -elektronskim strujama, što dovodi do aromatičnosti protonirane strukture. S druge strane, računi pokazuju da je subporfirin za samo 5 kcal mol^{-1} bazičniji od porfirina, što se može objasniti neplanarnošću takve strukture, uzrokovane manjom veličinom prstena.